SACLANTCEN Report SR - 110

SACLANTCEN Report SR - 110

SACLANTCEN Report SR - 110

SACLANT ASW RESEARCH CENTRE REPORT

LOGARITHMIC LEAST MEAN SQUARE SOUND-FIELD ESTIMATION

by

Walter M.X. ZIMMER

MARCH 1987

NORTH ATLANTIC TREATY ORGANIZATION

SACLANTCEN
LA SPEZIA, ITALY

Report no. changed (Mar 2006): SR-110-UU

NORTH ATLANTIC TREATY ORGANIZATION

SACLANT ASW Research Centre
Viale San Bartolomeo 400,
I-19026 San Bartolomeo (SP), Italy.

tel: national 0187 540111
international + 39 187 540111

telex: 271148 SACENT I

Report no. changed (Mar 2006): SR-110-UU

SACLANTCEN SR-110

LOGARITHMIC LEAST MEAN SQUARE SOUND-FIELD ESTIMATION

by

Walter M.X. Zimmer

March 1987

This report has been prepared as part of Project 02.
Date of submission: 28-July-1986

Approved for Distribution

Ralph R. Goodman
Director

CONTENTS

Report no. changed (Mar 2006): SR-110-UU

LOGARITHMIC LEAST MEAN SQUARE SOUND-FIELD ESTIMATION

by
Walter M.X. Zimmer

ABSTRACT

The report deals with narrowband beamforming techniques for Passive Sonar applications. In particular, the Least Mean Square parameter-estimation technique is used to determine the spatial sound-field power density. To find the optimal solution the steepest descent iteration has been selected in order to avoid computation-intensive matrix calculations. Comparisons have been made between the steepest descent and the so-called WB iteration, a technique which was developed some years ago at SACLANTCEN by R.Wagstaff and J.L.Berrou. The results of these two iteration procedures have been compared against the conventional beamformer using perfectly known data, simulated random data and real data. Also, a statistical performance analysis has been carried out to provide numerical evidence of the probability of detection and resolution, and of the accuracy of bearing estimation. In this context the two sound-field estimation techniques have been compared not only with the conventional beamformer but also with the Capon adaptive beamformer and the MUSIC orthogonal beamformer.

INTRODUCTION

In a previous report [1] it has been shown that high-resolution methods do not provide more accurate bearing estimates than the conventional beamformer. Also, when we deal with detection problems the conventional beamformer is in some sense optimal, whereas the high-resolution methods normally show decreased performance. An explanation of this non-optimal behaviour may be found in the observation that to achieve high resolution it is necessary to extrapolate the hydrophone cross-correlation function beyond the array aperture. This may be done without risk when the cross-correlation function is known exactly within the aperture. However, when the cross-correlation matrix is inexactly estimated within the aperture, its extrapolation may amplify the effect of the measurement errors. This in turn may increase the statistical uncertainty, yielding an increased standard deviation for the bearing and peak-level estimations.

When the traditional high-resolution methods do not meet the expectations of improved detection probability and accuracy of bearing estimation, then the question arises if there is some other possibility for increasing the resolution performance relative to the conventional beamformer without decreasing detection performance and accuracy of bearing estimation too much.

Normally, beamforming is applied when measuring the power of a source in a given direction and consequently the spatial power distribution can be taken as the quantity of interest. To measure this distribution in all of its details one would need an infinitely long array, which is not feasible: only finite arrays are realistic. To compensate for this deficiency the so-called high-resolution methods are applied, and effectively what all of these try to do is remove the effect of this spatial low-pass filter from the measured data. The result is a high-resolution image of the true spatial power distribution.

Because the effect of this spatial low-pass filter on the data is known a-priori, it seems reasonable to look for a method which allows us to use this knowledge directly.

This is precisely what is done with parameter estimation techniques. The most common of these techniques is the Least Mean Square (LMS) fit, but the so-called WB methods, which have been developed some years ago at SACLANTCEN by Wagstaff and Berrou [2,3,4] also belong to the same class of algorithm.

While it is rather easy to formulate the sound-field power estimation as a parameter estimation problem, its solution is not always clear and easy to achieve. In fact the WB algorithms are not yet understood in all of their details, and one of the motivations for this present analysis was the lack of detailed information about the WB algorithms and their performance figures.

To simplify the analysis the existence of more than one version (WB2,WB3,etc.) has been ignored and only the important principles behind the WB philosophy are used.

The outline of this report is as follows:

First we derive the model for the Least Mean Square procedure, where the model is equivalent to a conventional beamformer. After the definition of the optimality criterion the gradient iteration is presented and the necessary formulas are derived. Some computational procedures are then given, and the performance of the gradient iteration is presented via qualitative comparisons with the conventional beamformer. Next, the WB modification is introduced and the performance of the accordingly modified Least Mean Square problem is illustrated. The performance analysis compares the two sound-field estimation techniques with respect to detection and resolution probabilities and with respect to accuracy of bearing estimation. This comparison includes not only the conventional beamformer but also two other high-resolution techniques which were found appropriate for comparison: the Capon adaptive beamformer and the MUSIC orthogonal beamformer, the performance figures for which were taken from [1]. The Maximum Entropy Method has been excluded from the comparison due to its poor performance concerning detection and accuracy. Subsequent to the analysis some comments are made about the question: Why did it work? These comments illustrate some interesting aspects of the procedures.

1. DERIVATION OF THE MODEL

One of the most important aspects of the Least Mean Square fit is the model which we use to describe the measurements. In this report the sound field is modelled as a linear superposition of plane-waves. The difference between the model and the measurements taken from a linear array of hydrophones are used to estimate the parameters of the model.

The derivation of the model is based on the following assumptions:

i) The sound field to be measured can be modelled as a superposition of plane-waves.

ii) Different plane-waves are mutual uncorrelated.

iii) The measurements are performed using a line array with equidistantly spaced hydrophones.

iv) The measured data are narrowband-filtered so that beamforming via phase rotation is applicable.

Using assumption i) we may model the hydrophone measurements x_m as

$$x_m = \sum_{l=0}^{L-1} a_l e^{-2\pi i \frac{ml}{L}} \qquad m = 0, \ldots, M-1 \ , \tag{1}$$

where

M is the number of hydrophones,

L is the number of plane-waves,

a_l is the complex amplitude of the l-th plane-wave.

By virtue of this model the different plane-waves (sources) are assumed to be uniformly distributed in space according to a cosine scale. We further assume that the number of modelled plane-waves is much larger than the number of hydrophones: $L \gg M$.

Because we have assumed statistical independence of the plane-wave amplitudes a_l, and because $L \gg M$, we may interpret the ensemble of all a_l, i.e. $\{a_0, \ldots, a_{L-1}\}$, as the amplitude spectrum of the sound-field to be modelled.

Next we take these modelled measurements and go though a conventional beamformer process. As the result we get a modelled beamformer output, y_k

$$y_k = \sum_{m=0}^{M-1} w_m x_m e^{2\pi i \frac{mk}{K}} \qquad k = 0, \ldots, K-1 \,, \tag{2}$$

where

K is the total number of beams to be formed,
w_k is some hydrophone weighting coefficient.

We assume further that the total number of beams we intend to form is much larger than the number of hydrophones: $K \gg M$. However, it is not required that the number of beams coincides with the number of modelled plane-waves.

Inserting equation (1) into equation (2) we get a relation between the beams and the complex amplitude spectrum of the modelled sound-field

$$y_k = \sum_{l=0}^{L-1} a_l \sum_{m=0}^{M-1} e^{-2\pi i \frac{m(l-k')}{L}}$$

where $k' = k\frac{L}{K}$.

Next we model the beam power q_k as the averaged absolute square of the complex beam amplitude y_k

$$q_k = \langle |y_k|^2 \rangle.$$

where $\langle \cdots \rangle$ denotes the average.

Using now the assumption that different plane-wave amplitudes are uncorrelated, we may write

$$\langle a_l a_k^* \rangle = |a_l|^2 \rho(l = k), \tag{3}$$

where $\rho(\cdots)$ is a modified Kronecker symbol, which has the value unity when the expression within the brackets is true, and the value zero otherwise; the asterisk indicates the complex conjugate.

In consequence we get a linear relationship for beam power

$$q_k = \sum_{l=0}^{L-1} |a_l|^2 \left| \sum_{m=0}^{M-1} w_m e^{-2\pi i \frac{m(l-k')}{L}} \right|^2 . \tag{4}$$

Introducing the following abbrevations

$$b_l = |a_l|^2 \geq 0 \ ,$$
$$\Phi_{l,k} = \left| \sum_{m=0}^{M-1} w_m e^{-2\pi i \frac{m(l-k')}{L}} \right|^2 \ ,$$

we get a more compact notation for the modelled beam power,i.e.

$$q_k = \sum_{l=0}^{L-1} b_l \Phi_{l,k} \ . \tag{5}$$

In other words: the beam power is a linear combination of beam patterns $\Phi_{l,k}$ where the weighting factors are given by the power b_l of the individual plane-waves.

It is to be emphasized that the linearity of the model is based on assumption ii) which therefore becomes the fundamental assumption of the model as given in equation (4) or (5).

2. LEAST MEAN SQUARE FIT

In section 1 we modelled the power estimate of a conventional beamformer. The next step is to estimate the unknown power density b_l; $l = 1, \ldots, L-1$, of the sound-field.

The approach we will select is a Least Mean Square (LMS) fit of the modelled beam power to the measured values. This approach is appealing for at least two reasons. First the LMS philosophy is easy to understand, and second there is a related series of simple but nevertheless interesting algorithms in the literature. The basic idea of the LMS fit is to find a set of parameters which minimize the difference between the measurement (i.e. the beamformer power estimate p_k) and the model output q_k. For this it is necessary to define a difference measure between measurement and model.

Here we will not compare the quantities directly (linear difference) but will compare the logarithmic values. Consequently we define the Logarithmic Least Mean Square (LLMS) error E as

$$E = \sum_{k=0}^{K-1} (\ln p_k - \ln q_k)^2. \tag{6}$$

This transformation from the linear to the logarithmic difference is allowed, because in the presence of noise we may always assume that both p_k and q_k are positive. Such a difference measure is also used for the WB algorithms [2,3,4].

Also, because the logarithmic scale emphasizes small values, the transformation helps to make a better LMS fit for small measurement values.

To estimate the unknown sound-field density b_j we follow the standard LMS principle, where the optimal set of b_j is found when the LLMS error E becomes minimum:

Find b_j such that

$$E = \sum_{k=0}^{K-1} (\ln p_k - \ln q_k)^2 \longrightarrow \min \tag{7}$$

with the constraints

$$q_k = \sum_{j=0}^{L-1} b_j \Phi_{j,k}$$

and $\quad b_j \geq 0.$

We constrain the unknown parameters b_j to be non-negative so that they can represent the desired sound-field power density.

As it is of importance to get good estimates also at low values of b_j it is again convenient to solve the LLMS optimization with respect to the logarithm of b_j rather than b_j directly.

With this consideration the i-th component of the gradient of the LLMS error is given as

$$g_i = -2 \sum_{k=0}^{K-1} (\ln p_k - \ln q_k) \frac{\partial \ln p_k}{\partial \ln b_i}. \tag{8}$$

The necessary condition for the LMS error E to be minimum is that every component of the gradient vanishes. However, there is no direct and analytical solution of the resulting set of LLMS equations

$$g_i = 0; \qquad i = 0, \ldots, L-1 \,. \tag{9}$$

This is due to the high non-linearity within the equations (8).

The usual way to get the solution of (9) is to iterate from some starting point towards the desired optimal solution. The most common method is the so-called gradient method which is outlined in the next section.

The gradient iteration has the advantage that we can avoid the matrix calculation, which is almost unmanageable when we deal with an increased number of parameters and equations. In our case the size of the Hessian would be of the order of 1024×1024 entries.

3. GRADIENT ITERATION

3.1 Iterated Algorithm

Consider that we have some estimates of the parameters $c_j = \ln b_j$, which, however, do not solve the LLMS equations (9). The iterated gradient algorithm will construct a new estimate c'_j from c_j by first choosing a search direction d_j and then a step size α :

$$c'_j = c_j + \alpha d_j; \qquad j = 0, \ldots, L-1 \ ,$$

$$\text{or} \quad b'_j = b_j \exp(\alpha d_j). \tag{10}$$

If the new estimate of the sound-field density b'_j does not satisfy the set of LLMS equations (9), the iterated procedure (10) will be repeated.

As it is difficult to consider both choices simultaneously, we will first concentrate on the choice of d_j and then choose α such that the LLMS error E will be minimized for the selected search direction.

3.2 Steepest Descent

Given the value of the gradient vector g , a simple strategy is to choose the search direction along the steepest descent. Obviously the steepest descent direction is anti-parallel to the gradient g , i.e.

$$d_j = -g_j; \qquad j = 0, \ldots, L-1 \ . \tag{11}$$

It can be shown theoretically that if the step size is estimated in an optimal way, the steepest descent algorithm should converge to an optimal point from any starting point. However the method is very slow in practice, as the rate of convergence is only linear [5].

3.3 Optimal Step Size

Given a search direction d, the optimal step size is defined as the value of α that minimizes the LLMS error E for a fixed search direction:

Find α such that

$$E' = \sum_{k=0}^{K-1} \left(\ln p_k - \ln q'_k\right)^2 \longrightarrow \min$$

The necessary condition for E' to be minimum is that the derivative of E' with respect to the parameter α vanishes:

$$\frac{\partial E'}{\partial \alpha} = -2 \sum_{k=0}^{K-1} (\ln p_k - \ln q'_k) \frac{\partial \ln q'_k}{\partial \alpha} = 0,$$

where

$$\ln q'_k = \ln \left(\sum_{j=0}^{L-1} b_j e^{\alpha d_j} \Phi_{j,k} \right)$$

To approximate the term on the right side we write

$$\sum_{j=0}^{L-1} b_j e^{\alpha d_j} \Phi_{j,k} \approx e^{\alpha d_k} \sum_{j=0}^{L-1} b_j \Phi_{j,k}$$

which yields

$$\ln q'_k = \ln q_k + \alpha d_k$$

$$\text{and} \quad \frac{\partial \ln q'_k}{\partial \alpha} = d_k \quad ,$$

and therefore the derivative of the LLMS error E' with respect to α becomes

$$\frac{\partial E'}{\partial \alpha} = -2 \sum_{k=0}^{K-1} (\ln p_k - \ln q_k - \alpha d_k) d_k \ .$$

The approximation of the optimal step size is then given as

$$\alpha = \frac{\sum_{k=0}^{K-1} (\ln p_k - \ln q_k) d_k}{\sum_{k=0}^{K-1} d_k^2} \ . \tag{12}$$

3.4 Stopping Criterion

Because we only iterate towards the optimal solution of the LLMS fit problem, there is a need to decide when to stop the iteration.

The usual procedures is to stop:

when all components of the gradient become almost zero

$$\sum_{j=0}^{L-1} g_j^2 \leq \epsilon_0 \ ,$$

- when the number of iterations exceeds an upper limit

$$loop \geq loop_{\max} \ .$$

For reason of simplicity the programs within this report use only the second stopping criterion. Hereby the maximum number of iterations $loop_{\max}$ is chosen to be 20. This value was found to be sufficient to get a stable, final estimate of the parameters.

3.5 Uniqueness of the Solution

When applying an iterated procedure one is, in particular, concerned as to whether or not the result will be unique.

Obviously there is no unique solution. This is due to the assumption that the number of plane-waves we model is much larger than the number of hydrophones we use to measure the actual sound-field. Therefore we have an infinite number of solutions for the LLMS problem (7).

The most significant consequence of this is that the solution will depend on the selection of the starting value of the unknown parameter b_j.

3.6 Selection of the Starting Point

Let us now make some considerations about how to select the initial values for the sound-field power density b_j; $j = 0, \ldots, L-1$.

Due to the influence of the starting value on the quality of the final solution, we have to be carefull in choosing the initial conditions of the iteration.

Consider for the moment that we measure only uniform distributed (white) noise. The optimal LLMS solution should therefore be as flat as possibe. Since with the LLMS algorithm we try to estimate the noise power density, an acceptable starting value for the LLMS parameter will be a constant value for all sound-field power estimates.

Initial values:

$$b_j = \text{const}; \qquad j = 0, \ldots, L-1$$

It seems to be fail-safe to assume a constant starting vector also in those cases where we are dealing with real data and not uniform noise alone. We expect the algorithm to make corrections to the constant starting vector only for those components that correspond to

the directions of sound sources. With this specific choice of starting vector we select from all possible LLMS solutions the one which seems to add minimal new information to the measured one. Such a decision criterion is known to follow the maximum entropy principle [1].

3.7 Summary of the Gradient Iteration

Now having all components necessary for the LLMS fit gradient iteration it useful to summarize.

Model:

$$q_k = \sum_{l=0}^{L-1} b_l \Phi_{l,k} \quad ,$$

where

$$b_l = |a_l|^2 > 0$$

$$\Phi_{l,k} = \left| \sum_{m=0}^{M-1} w_m e^{-2\pi i \frac{m(l-k')}{L}} \right|^2 \quad .$$

LLMS error:

$$E = \sum_{k=0}^{K-1} (\ln p_k - \ln q_k)^2 \longrightarrow \min.$$

Gradient iteration:

$$\begin{aligned} b'_j &= b_j e^{\alpha d_j} \\ d_j &= -g_j \\ g_j &= -2 \sum_{k=0}^{K-1} (\ln p_k - \ln q_k) \frac{\partial \ln q_k}{\partial \ln b_j} \quad . \end{aligned}$$

Initial values:

$$b_j = \text{const.}$$

Optimal step size:

$$\alpha = \frac{\sum_{k=0}^{K-1} (\ln p_k - \ln q_k) d_k}{\sum_{k=0}^{K-1} d_k d_k} \quad .$$

What now remains to be done is to compute model and gradient efficiently.

4. COMPUTATION OF MODEL AND GRADIENT

4.1 Beampattern

To compute the model and gradient of the LMS algorithm, let us first consider the beampattern $\Phi_{l,k}$

$$\Phi_{l,k} = \left| \sum_{m=0}^{M-1} w_m e^{-2\pi i \frac{m(l-k')}{L}} \right|^2 .$$

Upon reordering terms, we easily get

$$\Phi_{l,k} = \sum_{n=1-M}^{M-1} r_n e^{-2\pi i \frac{n(l-k')}{L}} \tag{13}$$

$$r_n = \sum_{m=m1}^{m2} w_m w^*_{m-n} \tag{14}$$

$$m1 = \max(0, n)$$
$$m2 = \min(M-1, M-1+n).$$

The new function r_n can be interpreted as the auto-correlation of the array shading function w_m and the beampattern is then seen to be nothing other than the Fourier transform of the autocorrelation of the array shading function.

Equation (14) may be evaluated easily, in particular for small number of hydrophones and known shading coefficients. However the following procedure, which is based on the Fast Fourier Transform (FFT), seems to be more elegant.

$$r_n = \sum_{l=0}^{L-1} e^{2\pi i \frac{nl}{L}} \left| \sum_{m=0}^{M-1} w_m e^{-2\pi i \frac{ml}{K}} \right|^2 .$$

4.2 Model Estimation

To estimate the model q_k efficiently we proceed as follows:

Starting with the generic expression

$$q_k = \sum_{l=0}^{L-1} b_l \Phi_{l,k},$$

and using equation (13) and interchanging the order of summation we get, with $k' = k\frac{L}{K}$,

$$q_k = \sum_{n=1-M}^{M-1} r_n e^{2\pi i \frac{nk}{K}} \sum_{l=0}^{L-1} b_l e^{-2\pi i \frac{nl}{L}} \quad . \tag{15}$$

This means that we first perform a FFT on the sound-field power vector, then multiply the result with the autocorrelation function of the array shading, and finally perform an inverse FFT to get the modelled beamformer estimate.

The computational effort is essentially two FFTs and one vector multiplication.

4.3 Gradient Estimation

For the estimation of the gradient we consider equation (18)

$$g_j = -2 \sum_{k=0}^{K-1} (\ln p_k - \ln q_k) \frac{\partial \ln q_k}{\partial \ln b_j} \quad .$$

First we observe that we can rewrite the partial derivative as

$$\frac{\partial \ln q_k}{\partial \ln b_j} = \frac{b_j}{q_k} \frac{\partial q_k}{\partial b_j} = \frac{b_j}{q_k} \Phi_{j,k} \quad .$$

and consequently the j-th component of the gradient becomes

$$g_j = -2b_j \sum_{k=0}^{K-1} \frac{\ln p_k - \ln q_k}{q_k} \Phi_{j,k} \quad .$$

Again we use equation (13) to replace the beam pattern $\Phi_{j,k}$, and after interchanging the order of summation we get

$$g_j = -2b_j \sum_{n=1-M}^{M-1} r_n e^{-2\pi i \frac{nj}{L}} \sum_{k=0}^{K-1} \frac{\ln p_k - \ln q_k}{q_k} e^{2\pi i \frac{nk}{K}} \quad . \tag{16}$$

The computational procedure of the gradient is now equivalent to that of the LLMS model (two FFTs and two vector multiplications).

5. PRESENTATION OF THE LLMS SOUND-FIELD ESTIMATOR

To get a feeling for the characteristics of the LLMS sound-field estimation, we consider first the analytic case, where we apply the technique to perfectly known data. Second, we apply the technique to simulated (i.e. random) data. Third, we apply the technique to real data.

5.1 Analytical Data.

Consider the following scenario: The sound field which we want to estimate consists of four signals plus uniform distributed (white) noise. The characteristic quantities of the signals are summarized below:

Signal	Beam number	Bearing(deg)	Signal Power(CBF output)
1	300	65.54	20 dB
2	324	68.46	20 dB
3	348	71.32	20 dB
4	400	77.36	10 dB

The number of hydrophones M is 32, with an inter-element spacing of $\lambda/2$. The total number of beams K is 1024, and the total number of modelled plane waves L is also 1024.

In figure 1 the output of the conventional beamformer (CBF) is compared with the LLMS sound-field estimation. The CBF can be easily identified as the upper curve.

We can make the following observations:
The LLMS sound-field estimates do not exceed the levels given by the CBF. However, the output SNR of the LLMS method is increased with respect to the CBF. The noise estimate of the LLMS method is flat and therefore in agreement with the white noise scenario. The noise level estimated by the LLMS method is decreased by about 7 dB with respect to the CBF. The group of three signals is well resolved. The level of the fourth signal is slightly under-estimated.

What are the conclusions we can draw from these observations?
First of all we can say that the LLMS method is a high-resolution technique. There is an increased processing gain due to the increased number of sound-field directions. In fact the difference between the CBF and the LLMS method corresponds to the square-root of the ratio of the number of hydrophones to the number of sound-field directions. This may be interpreted as indicating that while the conventional beamformer has a processing gain of $\log M$, the LLMS method seems to have a processing gain of $\log M + \log \sqrt{L/M}$. This indicates that we are in fact estimating the spatial power density. As expected, the estimated peak levels correspond to the one estimated with the CBF. The decision to start

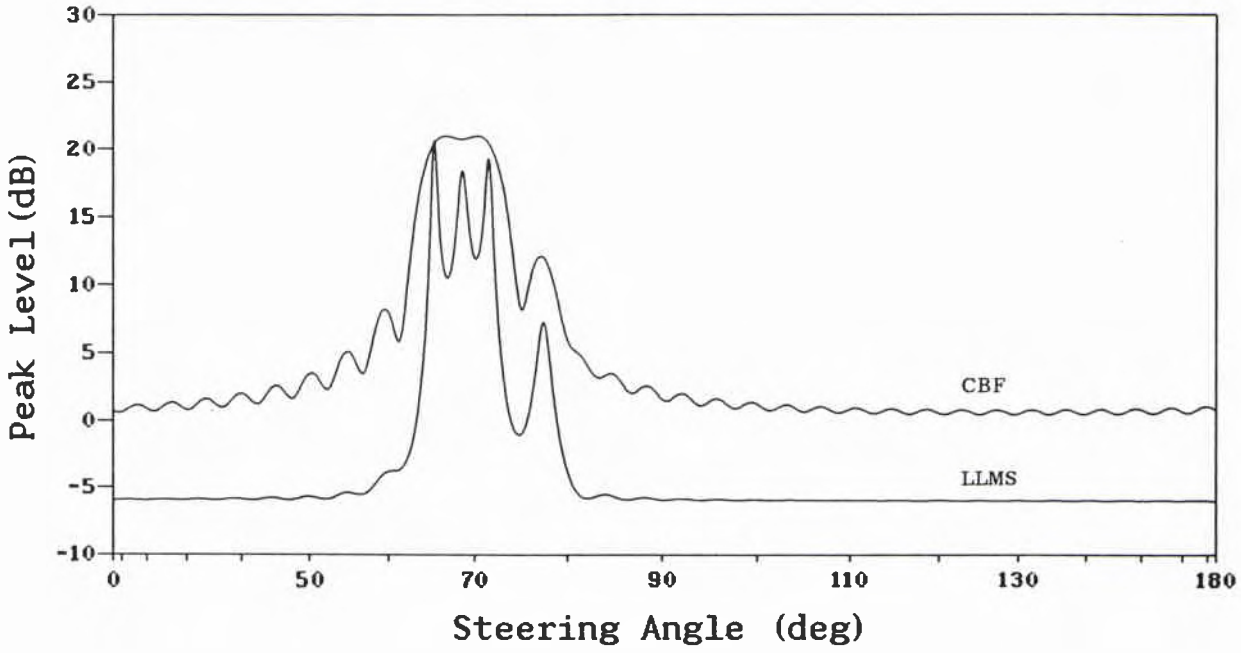

Figure 1: Comparison CBF and LLMS estimator; known data

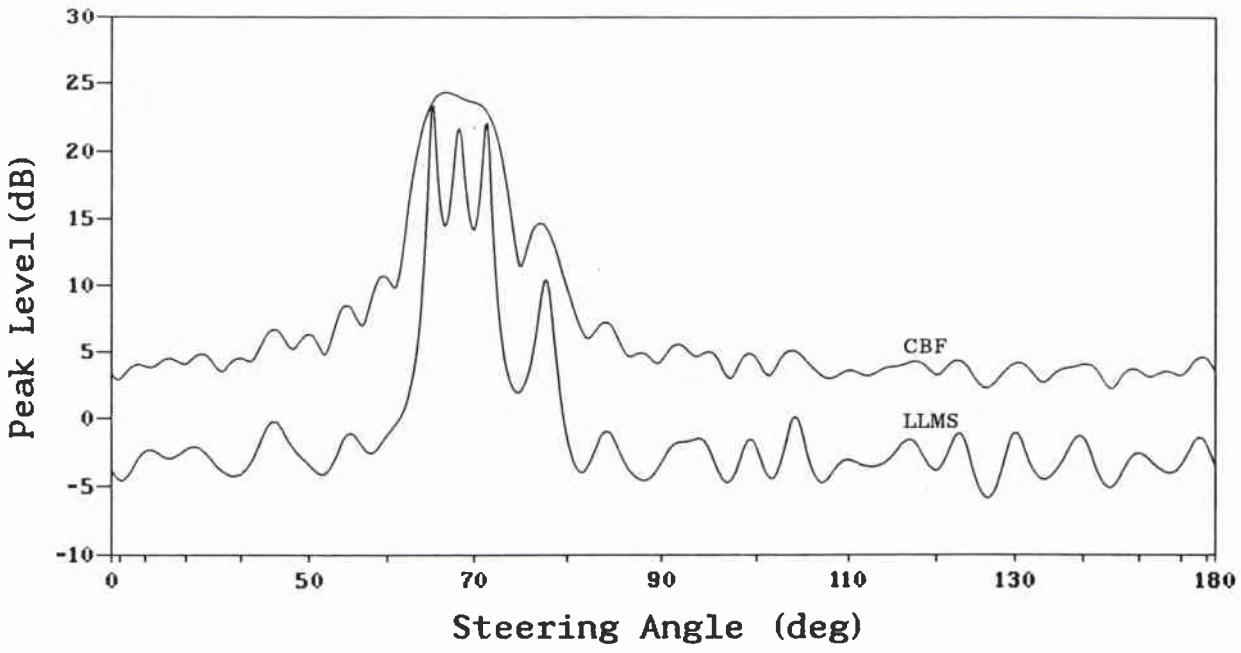

Figure 2: Comparison CBF and LLMS estimator; simulated data

the LLMS iteration with a uniform sound-field estimate may be seen as justified by the flatness of the final noise estimate.

5.2 Simulated Data.

In figure 2 the comparison between the CBF and the LLMS sound-field estimator is based on simulated data. For this case the cross-correlation matrix was estimated via an average of 40 single shots. The individual signals and the measurement noise were simulated as complex Gaussian variables and according to the scenario defined in the previous paragraph.

We observe that while the CBF cannot resolve the three bulk signals, the LLMS sound-field estimator clearly shows three peaks. However the estimated background noise of the LLMS method is rougher then the equivalent estimate of the CBF. The mean distance between the CBF and the LLMS background estimates is also here of the order of 7dB. The peak level of the weaker source is again slighly under-estimated.

5.3 Application to Real Data.

In figure 3 the CBF and the LLMS sound-field estimator are compared using real data.

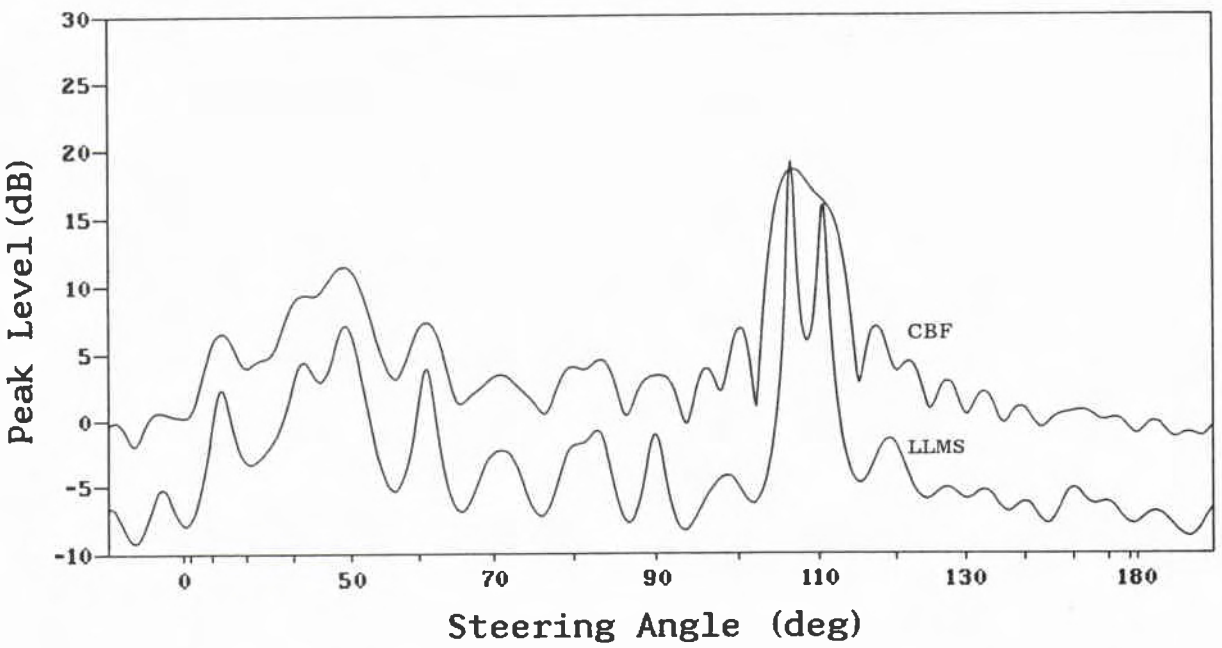

Figure 3: Comparison CBF and LLMS estimator; real data

Here, the comparison of the two techniques, CBF and LLMS, both using real data is somewhat problematical due to lack of exact knowledge of the sound field. However we may deduce some interesting features concerning the qualities of the LMS sound-field estimator.

For a better understanding of the figure it is revealed that the data have been recorded with the SACLANTCEN towed array system. The hydrophone data have been narrow-band filtered to allow beamforming via phase rotation. The selected frequency is slighly below the design frequency of the array and as a consequence the application of the FFT yields two areas of virtual beams located on the left and right sides of the beam pattern. The tow ship can be identified as the peak at 20 degrees. There are two closely spaced signals at about 110 deg.

First of all we observe that the LLMS method (lower curve) resolves the two sources at 110 deg. Comparing the peaks at 70 deg and 90 deg we find a broad LLMS estimate at 70 deg and a sharp one at 90 deg. This indicates that the LLMS method is able to describe properly not only plane-wave but also wide-angle signals.

Broad peaks correspond to non-planar waves produced by multipath, distributed sources or angular motion during the estimation of the cross-correlation matrix. It is clear that a single beampattern is not sufficient to identify the reasons for such beam broadening. To get an answer, the time history of the beam pattern must be taken into account. Also, the model assumption made in the beginning of this report is too simple to allow the analysis of the multipath structure of the sound-field propagation.

6. WB MODIFICATION

As mentioned in the introduction, one of the motivations for this report was the lack of understanding of the Wagstaff-Berrou (WB) algorithms which was developed at SACLANTCEN some years ago. In this section an attempt is made to formulate this class of algorithms in a more general way.

6.1 WB Generalization of the Search Direction

Consider the expression of the steepest descent search direction, which is given as :

$$d_j = 2 \sum_{k=0}^{K-1} (\ln p_k - \ln q_k) \frac{\partial \ln q_k}{\partial \ln b_j}.$$

To understand this equation better we first note that the correction of the j-th component of the sound-field level, $\ln b_j$, is proportional to d_j. Therefore we can say that the correction we make to the sound-field level is calculated as a weighted sum of the model-measurement mismatches. Here the weighting coefficients are given by the partial derivative of the

model with respect to the sound-field level we want to correct. Consequently a model-measurement mismatch will only contribute to a correction of the sound-field level when the partial derivative is high. In other words, the correction of the sound-field level takes into account only those components of the model-measurement mismatch that are important for the correction.

The WB correction of the sound-field level may be understood as a modification of the steepest descent algorithm, where the model-measurement mismatch is replaced by an effective one.

Steepest descent mismatch:

$$(\ln p_k - \ln q_k).$$

WB effective mismatch:

$$\sum_{l=0}^{K-1} g_{j,l}(\ln p_l - \ln q_l). \tag{17}$$

where

$$\sum_{l=0}^{K-1} g_{j,l} = 1 \qquad j = 1, \ldots, L-1 .$$

The WB modification uses as mismatch between model and measurement an average of the actual mismatches. The average itself depends on the component of the search direction.

With this modification the WB search direction becomes

$$d_j = 2 \sum_{l=0}^{K-1} g_{j,l}(\ln p_l - \ln q_l) \sum_{k=0}^{K-1} \frac{\partial \ln q_k}{\partial \ln b_j} \quad . \tag{18}$$

By selecting $g_{j,l}$ as the normalized partial derivative of the model with respect to the unknown parameters

$$g_{j,l} = \frac{\frac{\partial \ln q_l}{\partial \ln b_j}}{\sum_{k=0}^{K-1} \frac{\partial \ln q_k}{\partial \ln b_j}}$$

the WB search direction becomes the steepest descent.

In principle it should be possible to find the WB weights $g_{j,l}$ in such a way that they satisfy some optimality criterion, but no procedure of this type in yet known. There is more than one WB algorithm[2,3,4], but we will analyse only the last version known to the author, which is based on a computer listing of the program *FWWB4* [6]. Also, we concentrate on the estimation of the search direction and ignore the different selection of the initial estimate of the sound field.

6.2 WB Algorithm

To obtain the WB search direction we have to use as WB weights $g_{j,l}$ the normalized, squared partial derivative of the model with respect to the unknown parameters:

$$g_{j,l} = \frac{\left(\frac{\partial \ln q_l}{\partial \ln b_j}\right)^2}{\sum_{k=0}^{K-1}\left(\frac{\partial \ln q_k}{\partial \ln b_j}\right)^2} \quad . \tag{19}$$

It seems clear that with such a modification of the search direction we may find a qualitatively different result for the LLMS iteration. However, there is no proof that the result of the modified iteration is also a solution of the Least Mean Square fit problem as posed in section 2.

6.3 Presentation of the WB Method

6.3.1 Analytic Data

We consider the scenario to be the same one given in section 5, where the sound field that we wish to estimate is built up of four signals plus uniformly distributed (white) noise. The characteristic quantities of the signals are repeated below:

Signal	Beam number	Bearing(deg)	Signal Power(CBF output)
1	300	65.54	20 dB
2	324	68.46	20 dB
3	348	71.32	20 dB
4	400	77.36	10 dB

The number of hydrophones M is 32 with an inter-element spacing of $\lambda/2$. The total number of beams K is 1024, and the total number of modelled plane-waves L is also 1024.

In figure 4 the output of the CBF is compared with the result of the WB sound-field estimation. The CBF is easily identified as the upper curve.

We make the following observations:
The WB sound-field estimates do not exceed the levels given by the CBF. However the

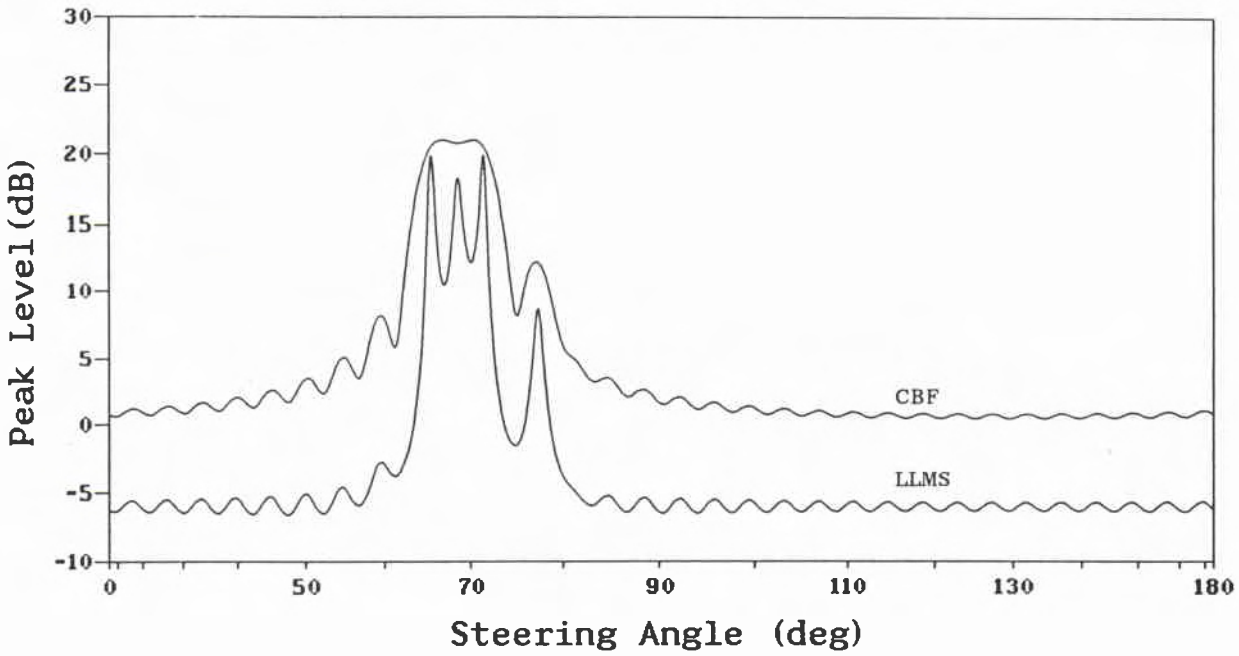

Figure 4: Comparison CBF and WB estimator; known data

output SNR of the WB method is greater than that of the CBF. The noise estimate of the WB method is not flat and therefore does not correspond to the white noise scenario. The noise level estimated by the WB method is about 7 dB less than that of the CBF. The group of three signals is well resolved. The level of the fourth signal is slightly underestimated.

What are the conclusions we can draw from these observations?
First of all we can say that the WB method is a high resolution technique. There is an increased processing gain due to the increased number of sound-field directions. However, the WB technique does not show a flat background noise estimate as we can observe for the LLMS method. Because the only difference between these two algorithms is the modification of the gradient, this imperfect noise estimate must be a consequence of this modification.

6.3.2 Simulated Data.

In figure 5 the comparison between the CBF and the WB sound-field estimate is based on simulated data. As in paragraph 5.2 the estimate of the cross-correlation is based on an average of 40 single shots and the scenario is the same as presented in the previous paragraph.

Comparing figure 5 and figure 2 we can say that the behaviour of the WB iteration and of the LLMS steepest descent iteration is quite similar. However a more detailed inspection

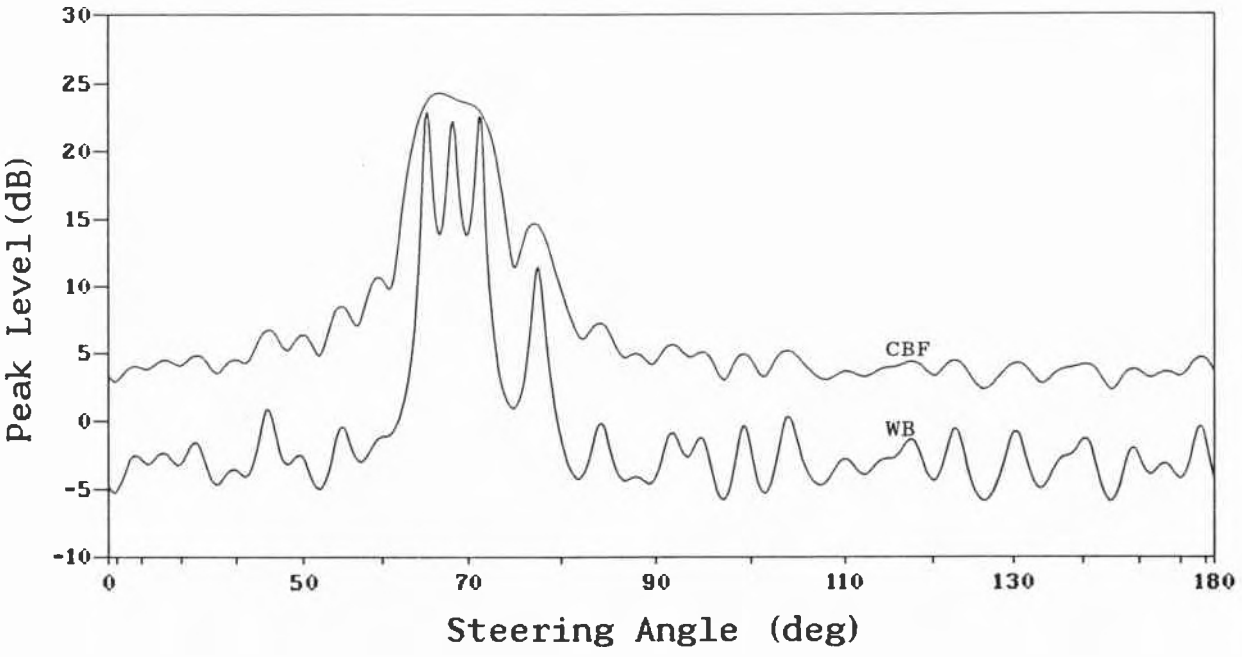

Figure 5: Comparison CBF and WB estimator; simulated data

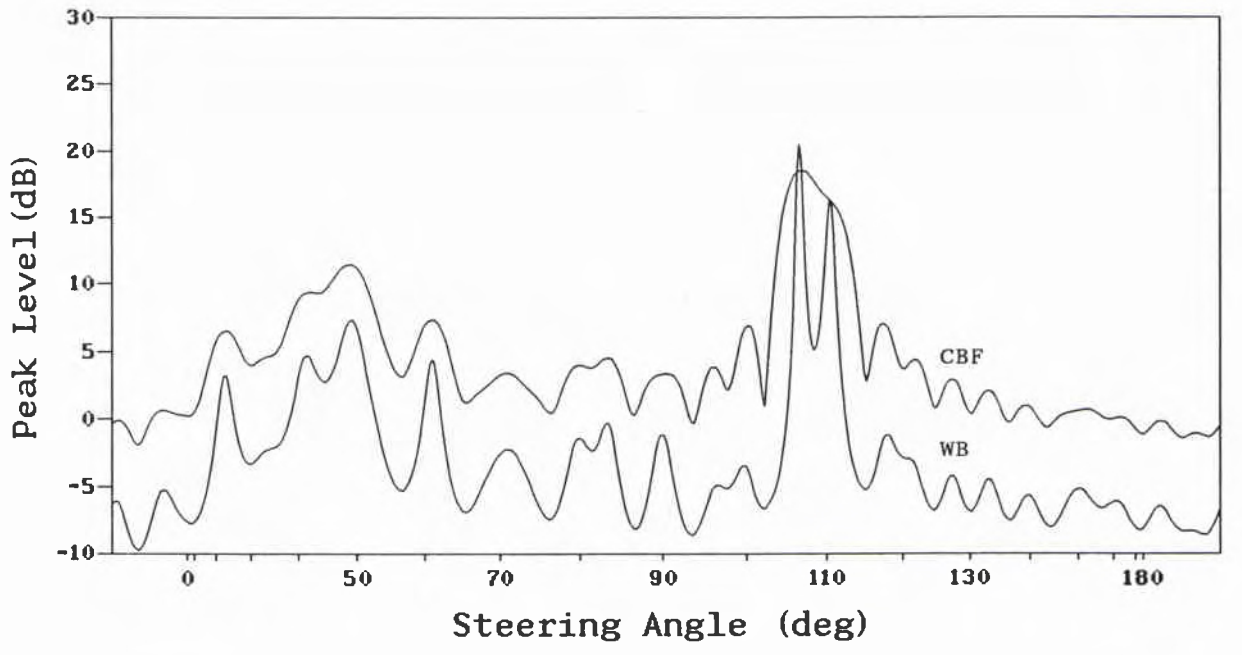

Figure 6: Comparison CBF and WB estimator; real data

reveals that the WB iteration produces slightly better separation of adjacent peaks. This is clearly due to the tendency of the WB iteration to oscillate. As consequences we can deduce that the WB iteration will produce slightly better resolution performance.

6.3.3 Application to Real Data

In figure 6 the CBF and the WB sound-field estimator are compared using real data. The snapshot used for this comparison is the same as in paragraph 5.3 .

Here again we can observe that the sound-field estimate produced by the WB iteration is quite similar to the one produced by the LLMS gradient iteration. There are no significant differences.

7. PERFORMANCE ANALYSIS

In the previous chapters we have seen in a qualitative way how the LLMS and the WB sound-field estimations behave with respect to the CBF. Here, we make some comparisons of a more quantitative nature. For this end an extensive statistical analysis bas been carried out, involving 1000 simulated measurements for each datum. To estimate the hydrophone cross-correlation function 32 hydrophones have been used and an average over 40 samples has been carried out.

Let us first consider the detection performance.
As in [1] a series of simulations has been carried out to get a statistical description of peak fluctuation. The detection probability has been estimated by comparing the distribution of the peak fluctuation of the signal plus noise case with the noise-alone peak distribution where the signal is absent. For this comparison the peak levels were measured in linear values and not with a logarithmic (i.e. dB) scale.

In figure 7 the detection probability of the two sound-field estimators is compared with not only the CBF but also with other high-resolution techniques: the Capon adaptive beamformer and the MUSIC orthogonal beamformer (Schmidt). The performance data for CBF, Capon and MUSIC were taken from [1].

In figure 7 the detection probability of a single source against white noise is plotted as a function of input SNR. Because the scenario assumed 32 hydrophones the conventional processing gain is about 15 dB. The abscissa is scaled according to a gaussian normal distribution and consequently a normal distributed detection probability would yield a straight line. The false alarm probability has been assumed to be 1.35×10^{-3}.

We observe that neither the LLMS-gradient nor the WB-iteration method performs better than the CBF. For increased SNR the detection performance of the WB iteration approaches the limit given by the CBF. The performance of the LLMS steepest descent iteration is slightly worse than that of the CBF but better than that of the Capon beamformer.

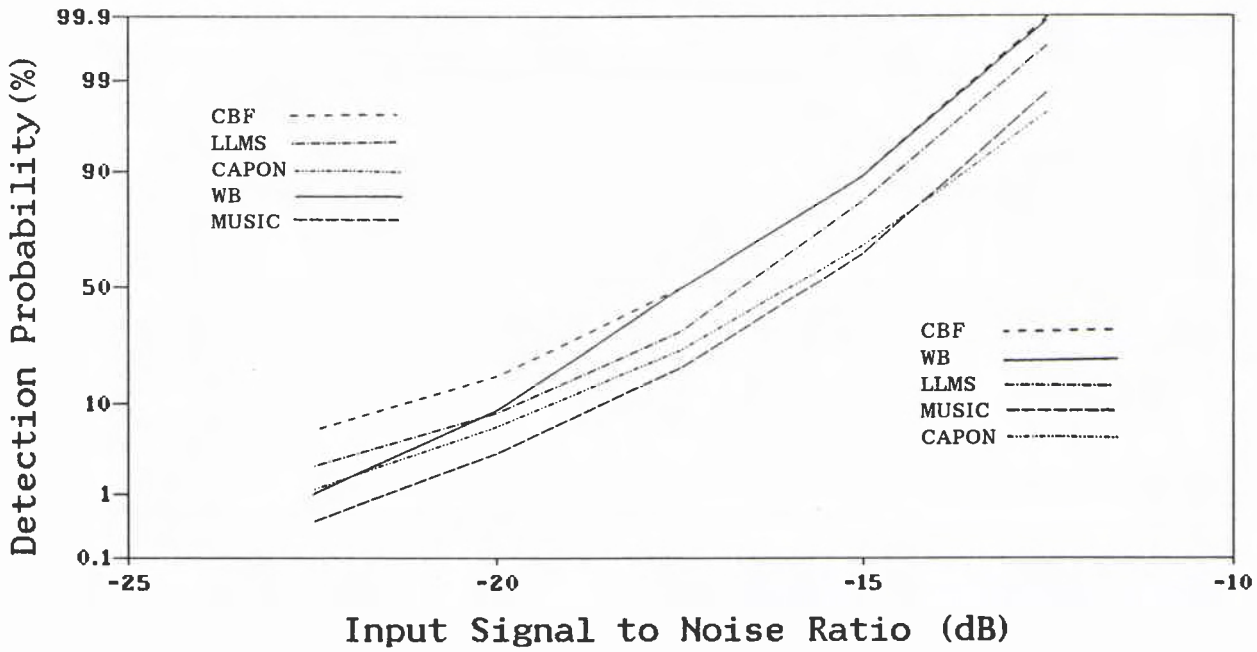

Figure 7: Probability of detection

In considering the resolution performance of the two sound-field estimation procedures, a different series of simulations was carried out: two individual signals with 0 dB input SNR were simulated at varying separations. The background was simulated white noise. The two sources were assumed to be resolved when there were two local maxima close to the simulated directions.

In figure 8 the probability of resolution has been plotted against the separation of the two sources. The abscissa is again scaled according to a gaussian normal distribution. The separation of the two sources is measured in units of reciprocal aperture (i.e. the conventional mainlobe width corresponds to 2 units).

From figure 8 we easily can see that the WB iteration performs better than the orthogonal beamformer MUSIC. The LLMS method performs worse than MUSIC but better than the Capon method.

Figure 8 clearly indicates that the two sound-field estimation techniques may be classified as high-resolution techniques.

The third component of the performance analysis is the accuracy of bearing estimation. Given the sharp peaks of high-resolution methods one might suspect that they can be used to estimate the source bearing more accurately than with the CBF, with its broad mainlobe. However this is not the case, as can be seen in [1]. It is therefore of interest to

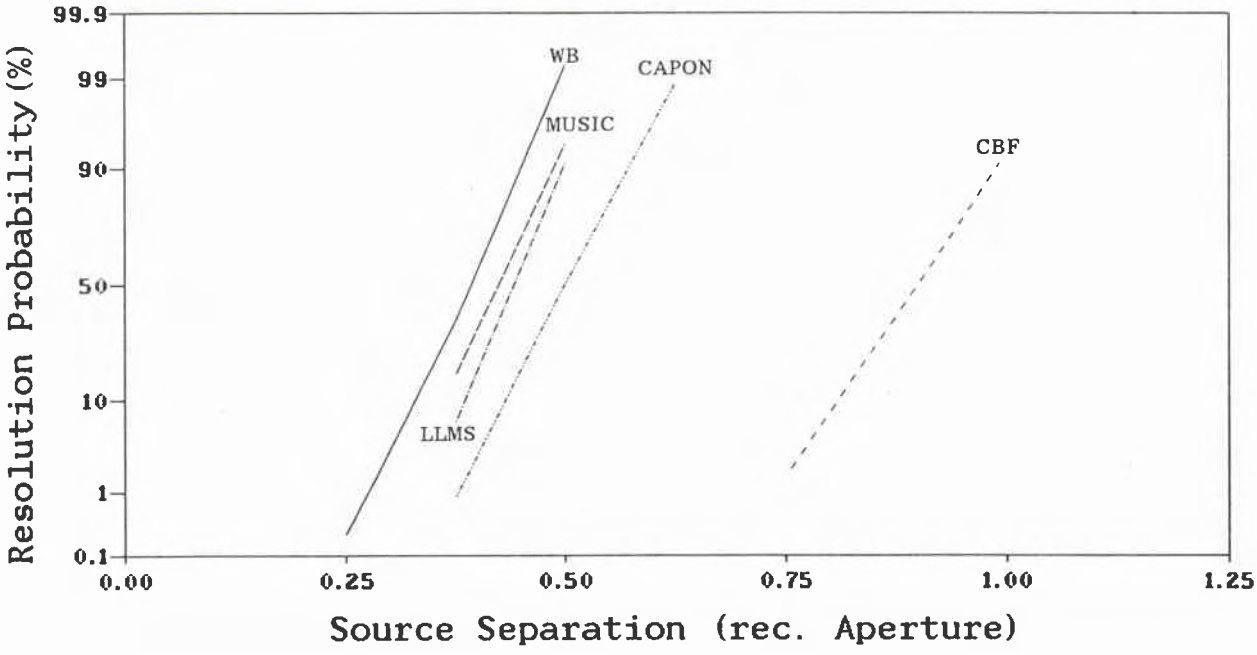

Figure 8: Probability of resolution

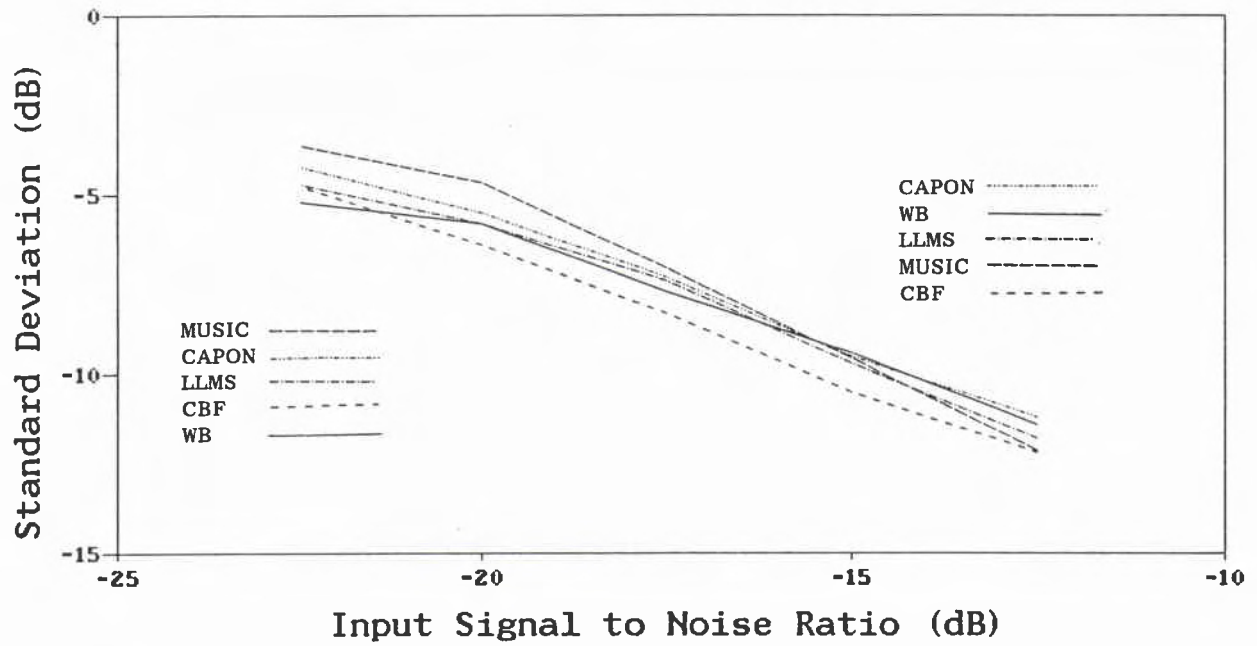

Figure 9: Accuracy of bearing estimation

see how the sound-field estimators perform in this respect.

In figure 9 the standard deviation of the bearing estimation is plotted as a function of input SNR. The standard deviation is normalized with respect to the reciprocal aperture.

From figure 9 we can see that the accuracy of the two sound-field estimators is no better than the accuracy of the CBF. To be more precise: the accuracy of the sound-field estimators is comparable to the accuracy of the Capon adaptive beamformer.

8. DISCUSSION

After having seen how the sound-field estimation procedures work and how well, it is worthwhile asking the question: Why did they perform so well?

i) Did we not throw away information by using the power output of the conventional beamformer as our model?

ii) Also: how can we estimate many more parameters (sound-field power values) than we have hydrophones available?

To the first question:

There was no throwing away of information such as the phase of the complex signal amplitudes. After assumption ii) of section 1 we assumed the complex amplitude of different sources to be uncorrelated. As a consequence only the hydrophone cross-correlation function is of importance for the beamforming concept and the power output of the beamformer is simply the Fourier transform of the hydrophone cross-correlation function. Because assumption ii) of section 1 holds for zero-mean random (stochastic) signals, we can deduce that for such signals the model we have constructed does not neglect important information.

To the second question:

The application of the LMS fit to problems does not result in an unique solution when there are more parameters than independent measurements. As a consequence, the selected algorithm should yield a solution which correponds as close as possible to the scenario of interest. The gradient iteration allows iteration from predefined initial values towards a possible solution. A constant vector chosen for the initial values is consistent with the lack of a-prori information about the final solution vector. Further, the gradient iteration procedure manipulates only measured information or information correponding to measurements. The selection of a logarithmic scale emphasizes small power values and is therefore more appropriate for the statistics of sonar signals. This is why it is not a surprise that we get a solution which corresponds more or less to the desired one.

However, there is a small residual problem concerning the speed of convergence. A detailed

observation of the estimated optimal step-size α revealed that the convergence did not approach zero even in cases where the sound-field estimate did not change very much. This was another reason for selecting the limitation of the number of iterations as the only stopping criterion.

Summary

The purpose of this report was twofold:
First, to show how the Least Mean Square parameter estimation technique may be used to estimate the spatial sound-field power density. It was hoped that it would also improve understanding of the WB iteration developed some years ago at SACLANTCEN. While it was not possible to get complete physical insight of the WB philosophy, it has nevertheless been shown that a simple connection can be achieved between the WB algorithms and the steepest descent iteration.

Secondly, to give quantitative evidence of the performance of the sound-field power estimation algorithms. This has been done by estimating the probability of detection and resolution together with the accuracy of bearing estimation. It can be clearly deduced from the results that the two sound-field power estimators belong to the better-performing high-resolution methods. In addition, it can be deduced from the performance figures that it may be possible to improve the overall performance (detection,resolution and accuracy) by modifying the classical steepest descent iteration. A possible way to go is closely related to the WB iteration, the difference being that the modification should not be made in an ad-hoc way but in an optimal way. This would also permit the inclusion of more a-priori information.

Because the detection performance is only slightly decreased with respect to the CBF, the two algorithms provide an interesting approach for obtaining high resolution where the signal-to-noise ratio is high and acceptable detection performance where it is low.

To summarize, one can say that Logarithmic Least Mean Square sound-field estimation is a powerful tool for incorporating a-priori information into the beamforming process. Knowledge of the filter characteristics of the finite array aperture has been successfully used to improve the resolution performance. It can be expected that the incorporation of further a-priori information may also improve the accuracy of the bearing estimate and the detection performance.

References

[1] Zimmer, W.M.X., High-Resolution Beamforming Techniques, Performance Analysis, SACLANTCEN SR-104. La Spezia, Italy, SACLANT ASW Research Centre, 1986.

[2] Berrou, J.L. and Boulon P., Une Nouvelle Methode Haute Resolution Rapide et Robuste, *Proc. GRETSI* 1983, 1015–1021.

[3] Wagstaff R.A. and Berrou J.L., A Fast and Simple Nonlinear Technique for High Resolution Beamforming and Spectral Analysis, *JASA* **75**, 1984, 1133–1141.

[4] Berrou, J.L. and Sandküler U., Iterative Deconvolution Algorithms for High Resolution Spectral Analysis and Beamforming, *Proc. GRETSI* , 1985, 385–390.

[5] Dixon L.C.W., Introduction to Numerical Optimisation, in ed: Dixon L.C.W., Spedicato E. and Szegö G.P. "Nonlinear Optimisation ,Theory and Algorithms," *Birkhäuser Boston*, 1980.

[6] Sandkühler U., personal communication, 1985.

KEYWORDS

ACCURACY OF BEARING ESTIMATION

CONVENTIONAL BEAMFORMING

CAPON BEAMFORMER

DETECTION PROBABILITY

GRADIENT ITERATION

HIGH-RESOLUTION BEAMFORMING

LEAST MEAN SQUARE FIT

LOGARITHMIC LEAST MEAN SQUARE FIT

MUSIC BEAMFORMER

PARAMETER ESTIMATION

RESOLUTION PROBABILITY

SOUND-FIELD POWER ESTIMATION

STEEPEST DESCENT

WB ITERATION

Report no. changed (Mar 2006): SR-110-UU

INITIAL DISTRIBUTION

MINISTRIES OF DEFENCE	Copies
JSPHQ Belgium	2
DND Canada	10
CHOD Denmark	8
MOD France	8
MOD Germany	15
MOD Greece	11
MOD Italy	10
MOD Netherlands	12
CHOD Norway	10
MOD Portugal	2
MOD Spain	2
MOD Turkey	5
MOD U.K.	20
SECDEF U.S.	68

NATO AUTHORITIES	
Defence Planning Committee	3
NAMILCOM	2
SACLANT	10
SACLANTREPEUR	1
CINCWESTLANT/COMOCEANLANT	1
COMSTRIKFLTANT	1
COMIBERLANT	1
CINCEASTLANT	1
COMSUBACLANT	1
COMMAIREASTLANT	1
SACEUR	2
CINCNORTH	1
CINCSOUTH	1
COMNAVSOUTH	1
COMSTRIKFORSOUTH	1
COMEDCENT	1
COMMARAIRMED	1
CINCHAN	3

SCNR FOR SACLANTCEN	Copies
SCNR Belgium	1
SCNR Canada	1
SCNR Denmark	1
SCNR Germany	1
SCNR Greece	1
SCNR Italy	1
SCNR Netherlands	1
SCNR Norway	1
SCNR Portugal	1
SCNR Turkey	1
SCNR U.K.	1
SCNR U.S.	2
SECGEN Rep. SCNR	1
NAMILCOM Rep. SCNR	1

NATIONAL LIAISON OFFICERS	
NLO Canada	1
NLO Denmark	1
NLO Germany	1
NLO Italy	1
NLO U.K.	1
NLO U.S.	1

NLR TO SACLANT	
NLR Belgium	1
NLR Canada	1
NLR Denmark	1
NLR Germany	1
NLR Greece	1
NLR Italy	1
NLR Netherlands	1
NLR Norway	1
NLR Portugal	1
NLR Turkey	1
NLR UK	1

Total initial distribution	248
SACLANTCEN Library	10
Stock	22
Total number of copies	280